University of North Carolina Asheville
Journal of Undergraduate Research
Asheville, North Carolina
December 2018

# Synthesis and Antibiotic Evaluation of Bedaquiline Analogs in Complex with *E. coli's* Gram-Negative $F_1F_0$-ATP Synthase

Alexander M. Hanamean
Department of Chemistry
University of North Carolina Asheville
One University Heights
Asheville, NC28804 USA

Faculty Advisor: Dr. Amanda Wolfe and P. Ryan Steed

## Abstract

Bedquiline (BDQ), a novel antibiotic, significantly inhibits the $F_0$ c-ring of F-ATP synthase (F-ATPase) in drug resistant *M. tuberculosis* through steric hindrance and stops ATP production, thereby facilitating cell death However, due to differences in amino acid sequence, binding affinity of BDQ to the F-ATP synthases of other bacteria are significantly reduced. Primarily targeting Gram-negative *E. coli*, analogs of BDQ were synthesized to determine the efficacy of distinct functional groups to create the most potent analog. By changing the position of the hydroxy group to C1 instead of C2, to account for the changes at amino acid position 65 – Glu65→Asp65, it is theorized that binding will be enhanced. Synthesized analogs' potency were determined via inside-out vesicle $H^+$ pumping and bacterial assays.

## 1. Introduction

In the US, at least 2 million people and 23,000 deaths are recorded every year due to antibiotic resistant strains of bacteria.[1] As a growing issue, especially in developing countries due to reduced treatment options, resistance occurs through the overuse of antibiotics. An infection is treated, the bacteria causing the infection are killed, and resistant mutant bacteria remain, spread, and lead to the development of antibiotic-resistant bacterial strains. For instance, penicillin, first discovered in 1928, was rampantly used to treat the wounded soldiers of WWII. The first resistant strain was isolated in 1940, and development of other antibiotics were undertaken.[2] These studies led to the discovery of superbugs such as methicillin-resistant *Staphylococcus aureus* (MRSA), found in 1962, penicillin-R *Pneumococcus*, 1965, vancomycin-R *Staphylococcus aureus*, 2002, and others. Frustratingly, resistance can be transferred to non-resistant bacteria through horizontal gene transfer (HGT) causing the ever-present pressure for new-novel antibiotics to increase.[3]

Gram-negative and Gram-positive are a classification system developed by Hans Christian Gram in 1884 while looking at lung tissues. He added a stain to help visualize the bacteria easier and those that took-up the dye were dubbed Gram-positive and those that didn't Gram-negative. Gram-negative bacteria have an additional phospholipid bilayer creating an extra periplasmic space (Figure 1). The additional cell wall and periplasmic space, in conjunction with a very robust drug efflux system, make drug delivery to and penetration of bacteria more difficult to treat and develop. Some common Gram-negative bacteria include but are not limited to: *Escherichia coli* (*E. coli*), *Acinetobacter baumanii* (*A. baumanii*), *Pseudomonas aeruginosa* (*P. aeruginosa*), *Klebsiella pneumoniae* (*K. pneumoniae*), *and Neisseria gonorrhoeae* (*N. gonorrhoeae*).

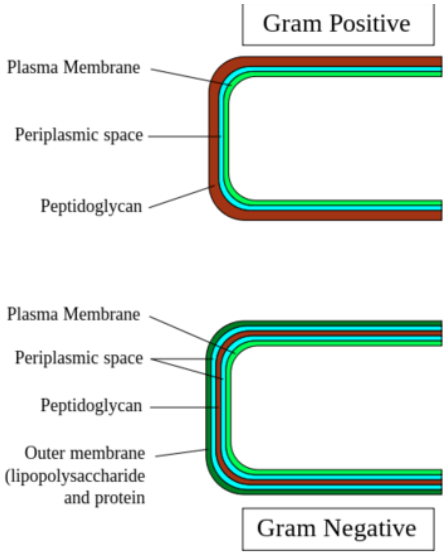


Figure 1. Cellular membrane differences between Gram-positive and Gram-negative bacteria.[4]

Tuberculosis (Tb) is a deadly and difficult to treat bacterial infection resulting in 10.4 million infected and 1.7 million deaths worldwide in 2016.[5] Caused by *Mycobacterium Tuberculosis*, a gram-negative mycobacteria, it mainly affects the lungs but can spread to the pleural membrane, bones, and central-nervous, lymphatic, and genitourinary systems. Due to slow growth, it can lie dormant for years in its latent form, keeping patients asymptomatic. Roughly 10% of those infected become symptomatic, and of those not well-treated, the death rate is 66%. HIV, immunocompromised, severely sick, and elderly patients are more likely to become symptomatic. The greatest frequency of Tb patients are found in developing countries as access to suitable antibiotics has been slow.

Discovered in 2005, Bedaquiline (BDQ, Figure 2a) showed strong antibiotic potential against drug and multi-drug resistant tuberculosis (MDR-Tb), was FDA approved in 2012, and placed on the market under the generic name Sirturo. BDQ falls under a new drug classification of diarylquinolines (DARQs), which are highly effective against Tb through the inhibition of $F_1F_0$-ATP synthase's c-ring rotation.[6–11] As an oral drug, BDQ has a strong pharmacokinetic (PK) profile with minimum inhibitory concentrations (MIC) and concentration at 50% inhibition ($IC_{50}$) values at 0.010 μg/mL (ppm) and 20-25 nM respectively. The $T_{max}$, the time at which $C_{max}$, the highest concentration of an administered drug in plasma is attained, of BDQ is ~1 hour and the half-life ($T_{1/2}$) 43.7 – 64 hours in plasma and 28.1 – 92 hours in tissue showing that BDQ is absorbed and distributed quickly and metabolized and excreted slowly (Figure 2b).[6] Doctors tend to not prescribe BDQ more frequent than 5 doses/week to reduce the chance of BDQ-resistant strains to develop and keep patients from developing unwanted side effects.

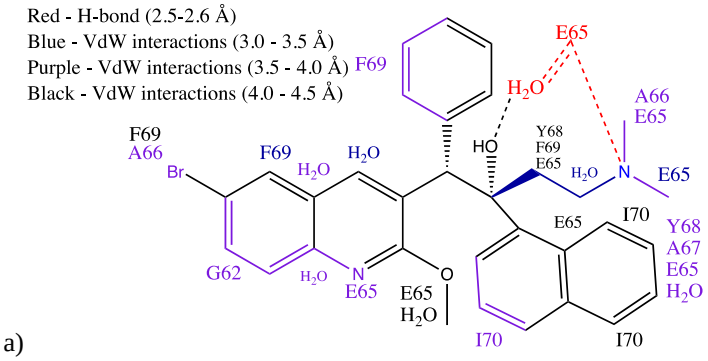


a)

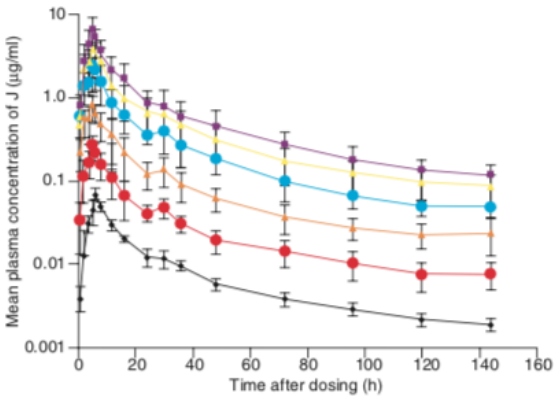


b)

Figure 2 (a) The structure of BDQ with respective amino acid structural interactions.[6] (b) Pharmacokinetic profile of BDQ (Black diamonds: 10 mg; red circles: 30 mg; Orange triangle: 100 mg; blue circles: 300 mg Yellow triangles: 450 mg; purple squares: 700 mg).[6]

Adenosine triphosphate (ATP) is a molecular energy carrier used by a variety of cellular systems and is essential for survival. Hydrolyzed via metabolic pathways, ATP is broken down into either adenosine diphosphate (ADP) or adenosine monophosphate (AMP), releasing a significant amount of energy for systematic cellular use (~30.5 kJ/mol). $F_1F_0$-ATP synthase (F-ATPase, Figure 3) is a membrane-bound protein that uses molecular motion via $H^+$ pumping, condenses ADP/AMP and $P_i$ back into ATP, and release the newly formed energy carrier into the cell. It is divided into two domains: $F_1$ and $F_0$. The $F_1$ domain is further divided into 5 subunits: α, β, γ, δ, and ε; whereas, the $F_0$ domain is split into 3 subunits: a, b, and c. The $F_1$ γ-subunit forms the main stalk, connecting the $F_1$ and $F_0$ domains. External periplasmic (P-side) $H^+$ ions are pumped through the a-subunit into the cytosol (N-side) through interactions with the a-subunit's Arg210 residue and the c-ring's Asp61 reside, generating rotation of the c-ring. Every 120° rotation of the c-ring, respectively rotates the main γ stalk, conformationally changing the $F_1$-α and β-subunits where ADP/AMP and $P_i$ bind, continued conformational changes catalyze the reformation of ATP, and is then released back into the cell for later use. Without F-ATPase, cellular functions would stop as no more energy would be available for use.

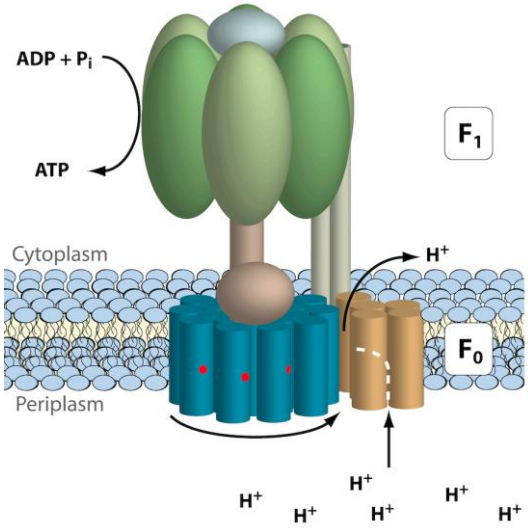


Figure 3. General structure of F-ATPase divided into its sub-regions and units.

BDQ's mechanism of action (MOA) begins with the dimethylamine group inserting itself into the c-ring binding site and having strong hydrogen-bonding interactions with residue Glu65. Phe69 then changes conformation, reducing

steric hindrance between the c-ring and BDQ; the naphthalene group acts as a hydrophobic platform that pushes BDQ further into the binding site and allows the hydroxyl group to form hydrogen-bonds with the Glu65 residue using one of two imbedded water molecules as an intermediate (Figure 2a, 4). Once attached, BDQ comes into contact with the a-subunit and stops rotation through steric hindrance, and action of the F-ATPase molecular motor. Without rotation, new c-ring Asp61 residues cannot come into contact with a-subunit Arg210 residues and complete ion-exchange to facilitate rotation; additionally, stopping $H^+$ pumping. Without rotation, the γ-main stalk cannot cause conformational changes to the α and β subunits; ADP and $P_i$ do not bind and ATP production ceases.[6–8,12,13]

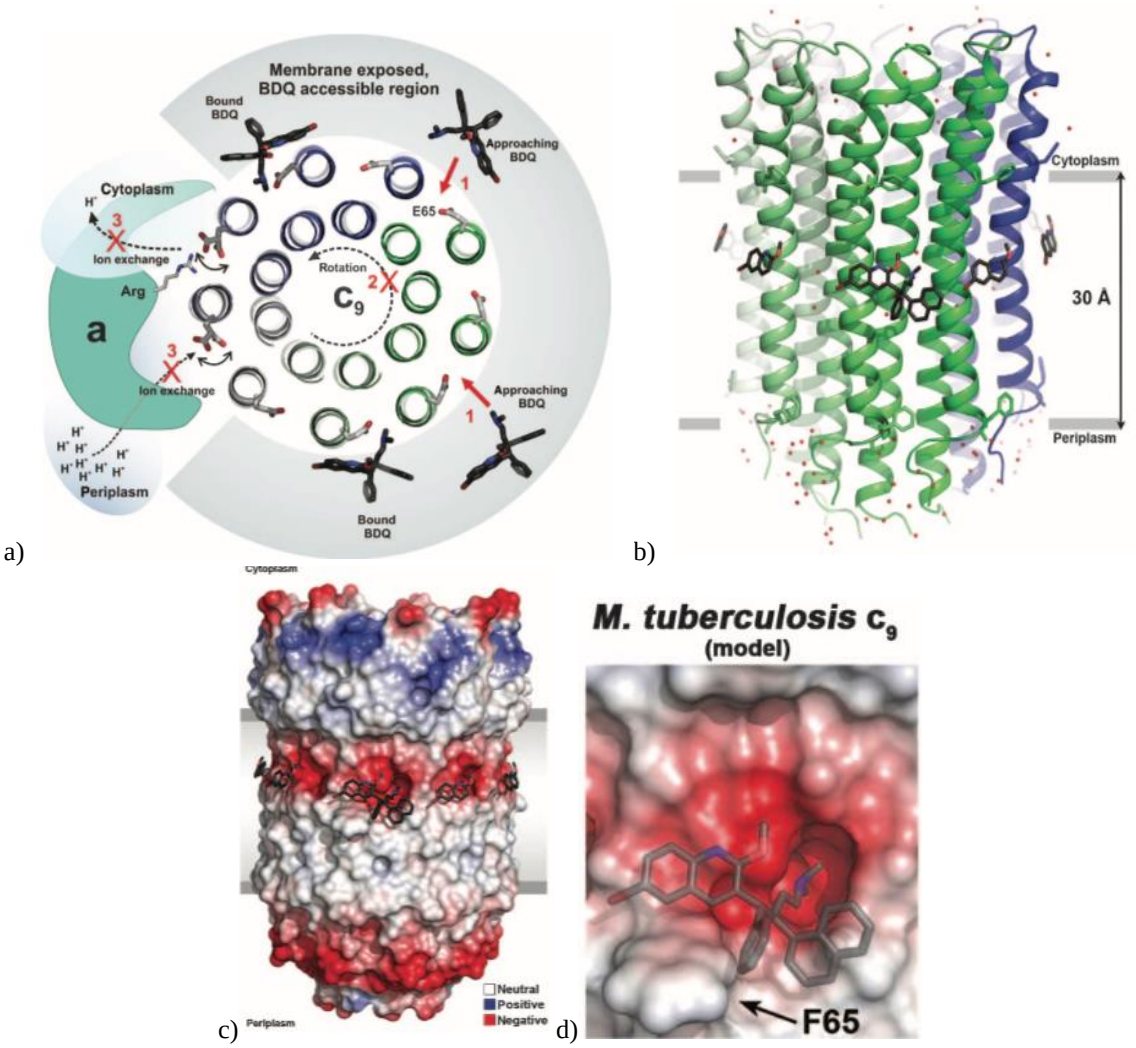


Figure 4: BDQ mechanism and structural conformation of binding.

Figure 4 (a) Mechanism of BDQ binding. (b) Cartoon depiction of structural BDQ binding to F-ATPase's c-ring. (c) 3D electrostatic potential distribution of the F-ATPase c-ring and BDQ binding. Membrane borders are indicated by gray bars. (d) Close-up of BDQ binding pocket.[6–8]

BDQ is highly selective for Tb due to the differences in amino acid sequences. Not surprisingly, the BDQ $IC_{50}$ value of *E. coli* versus Tb is insignificant in comparison (>32 μg/mL vs. 0.010 μg/mL respectively).[7] With noteworthy interactions occurring at residues 32, 63, 65-70, and 72 (Figure 2a & 5), the change at residue 65 has the greatest effect on binding (Glu65 to Asp65) to. With only a single carbon chain length shorter, a lone alkyl group can have large steric effects on drug-protein interactions. This study aims to synthesize analogs of BDQ that will complex with *E.*

*coli's* $F_1F_0$-ATP synthase by considering the differences in amino acids and reducing hindrances of binding; steps will be taken to avoid interactions with human F-ATPase (ATP5G1, Figure 5). To account for the Glu65/Asp65 difference, the hydroxyl group is moved one carbon closer (C1) to the quinoline ring system so as to increase binding affinity. The hydroxyl and dimethylamine groups will be retained throughout the analogs as they hold the strongest interactions.

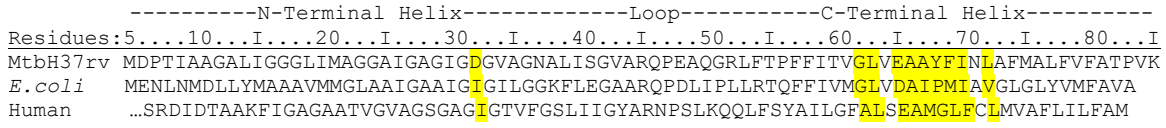


Figure 5. Comparative amino acid residues between *Mycobacterium tuberculosis* (MtbH37rv*), Escherichia coli* (*E. coli*), and Human ATP synthase (ATP5G1). Highlighted in yellow are residues involved in BDQ coordination.[7]

## 2. Results and Discussion

Analog synthesis was undertaken through multiple iterations of synthetic schemes and reaction conditions. The methoxy substitution methodology was quickly determined through trial and error of procedural order. High yield procedural confirmation of 2-methoxyquinoline-3-carbaldehyde (**2)** was conducted and finalized. The Grignard product **3** proved difficult to purify. Low yields are attributed to small amounts of 4-bromo-*N*,*N*-dimethylbutamine (**5**) synthesized, impurities, and side reactions (Scheme 1). For methodological development of **4**, a pyrrolidine substitution was substituted as pyrrolidine has greater sterics and, will therefore, have a greater likelihood of interaction with 1-bromo-4-chloropropane (Scheme 2). Three reaction conditions were tested: THF, DMF, and DMF/$K_2CO_3$. The DMF/$K_2CO_3$ reagent conditions were deemed the most successful under crude NMR. To increase yields, reactions normally run at room temperature (RT) could be refluxed instead. Synthesis characterization and confirmation were conducted through nuclear magnetic resonance (NMR) spectroscopy, Infrared (IR) spectroscopy, and liquid chromatography in conjunction with mass spectroscopy (LC-MS).

For the dimethylamine substitution of 1-bromo-4-chloropropane, selectivity of the chlorine substitution could not be assured. The dimethylamine group would more likely substitute the bromine group as it is a more reactive leaving group. Grignard reaction yields tend to be lower when done with chlorine instead of bromine; therefore, the synthetic scheme underwent an overhaul (Scheme 3). The methoxy, Grignard, and dimethylamine substitutions/additions would be conducted in that order respectively. Visualization, purification, and yields of **6** through Scheme 3 were proving to be unsuccessful. It was suggested to try a one-pot.

The one-pot was run under the same conditions as previous reactions, without the removal of any solvents during transfer (Scheme 4). The one-pot was unsuccessful as characterization was not observed and purification attempts were thwarted. A different procedure and acid-base work-up were proposed and conducted (Scheme 5). After synthesis, LC-MS determined the product (**6**) was present. The dimethylamine substitution was then redone with LC-MS confirmation. Procedural confirmations were deemed successful and the base pharmacore (**5**) was fully characterized.

Scheme 1. Synthesis of **5** and base structure for future analogs. Low percent yields are attributed to impurities, side reactions, or incomplete purification of products.

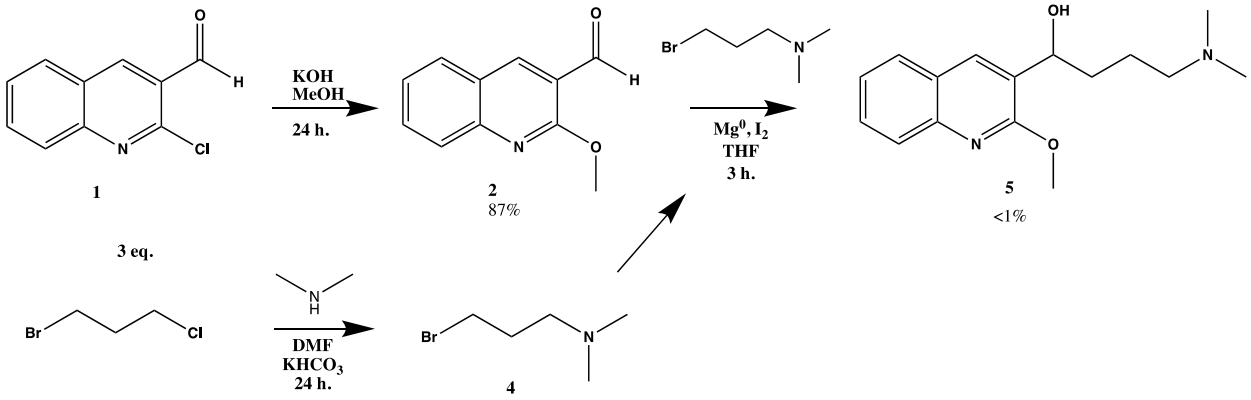


Scheme 2. Pyrrolidine substitution to set precedence for future dimethylamine substitution. All reactions were performed under dry conditions. (X1- THF; X2- DMF; X3- DMF, $KHCO_3$). Reaction condition X3 was deemed successful under crude NMR.

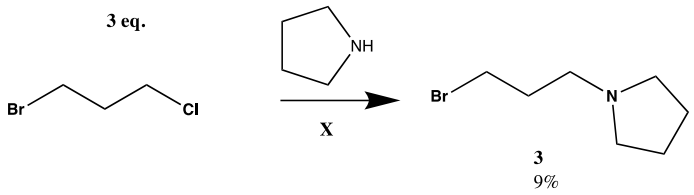


Scheme 3. Synthesis of **6** with Grignard addition preceding the dimethylamine substitution. Purification was not successful. H-NMR hints that **6** was successfully synthesized.

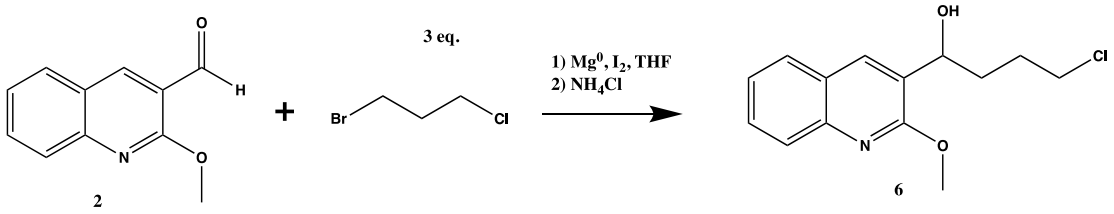


Scheme 4. One pot addition/substitution. Grignard addition completed first then added to dimethylamine solution to complete base analog **5** but proved to be ineffectual as well**.**

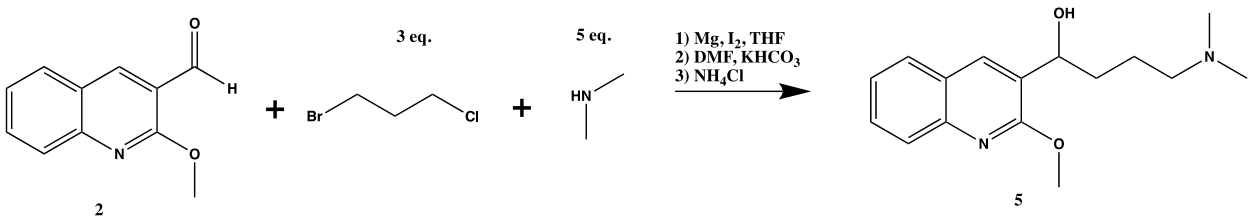


Scheme 5. Procedural and work-up changes were conducted. Synthesis was confirmed through LC-MS.

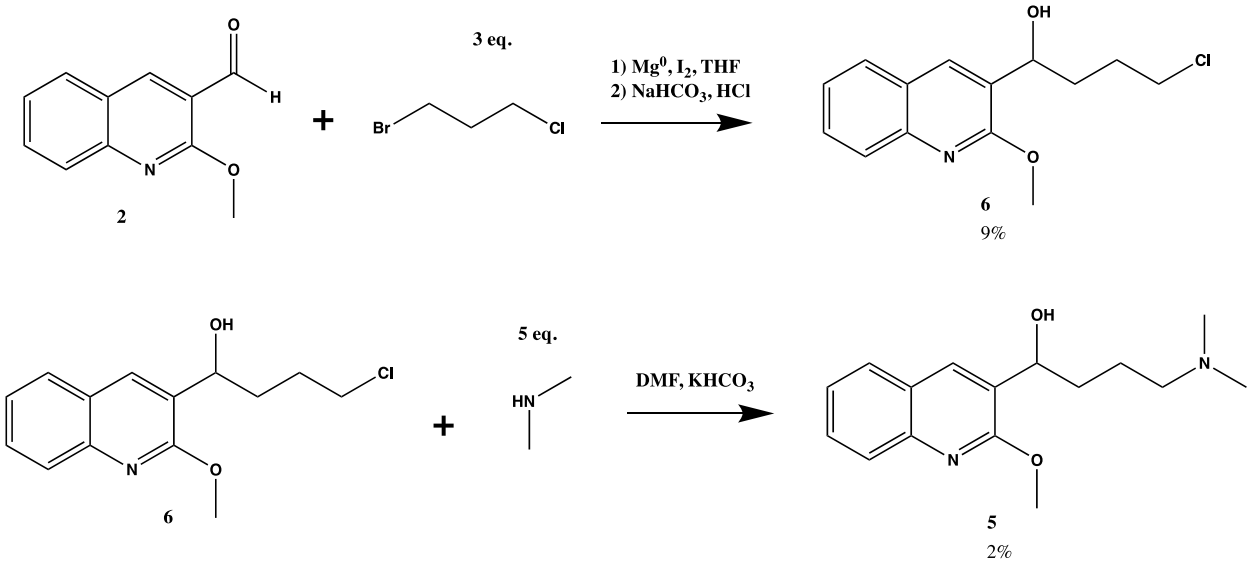


## 3. Fluorescent $F_1F_0$-ATP Synthase Activity Assay

ATP-driven proton pumping assays were conducted with *E. coli* inside-out (ISO) vesicles and evaluated through fluorescent spectroscopy via an AMINCO Bowman Series 2 Luminescence Spectrometer. Mixed solutions of F-ATPase ISO vesicles and tested compounds fluoresce due to 9-amino-6-chloro-2-methoxyacridine (ACMA), a fluorophore.[15] ACMA is taken into the vesicle and as $H^+$ ions are pulled into the vesicle via F-ATPase, ACMA is protonated and no longer fluoresces. Therefore, if F-ATPase is functioning, in an inverse relationship, the fluorescence is reduced, or quenched. ATP is added to the solution of F-ATPase and inhibitory compound at 20 s to induce rotary function and subsequent $H^+$ pumping. Eighty second later (100 s), Nigericin, a general antibiotic and ionophore, is added to the solution, collapsing the proton gradient and returning fluorescence to the sample. Reduced quenching indicates that synthesized analogs have anti-F-ATPase activity.

A F-ATPase activity assay was conducted with BDQ to establish a control (Figure 6a). All standards except the 100 nM sample followed the prediction of lower concentrations having less inhibition. The distinct difference is assumed be human error. While extremely low % yields of **5** were synthesized, there was enough product to test in the assay. **5** showed no inhibitory effects except the concentration 10 μM (Figure 6b). The 10 μM sample follows no trend and is therefore assumed to stem from human error as well.

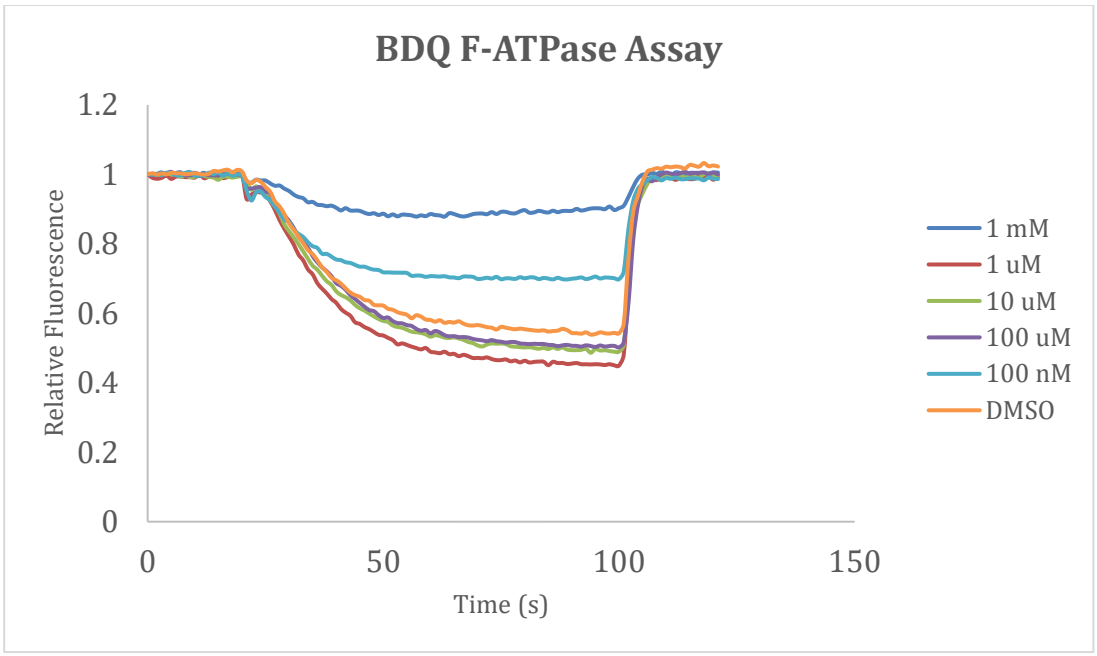
BDQ F-ATPase Assay
Relative Fluorescence
1.2
1
0.8
0.6
0.4
0.2
0
0
50
100
150
Time (s)
1 mM
1 uM
10 uM
100 uM
100 nM
DMSO

a)

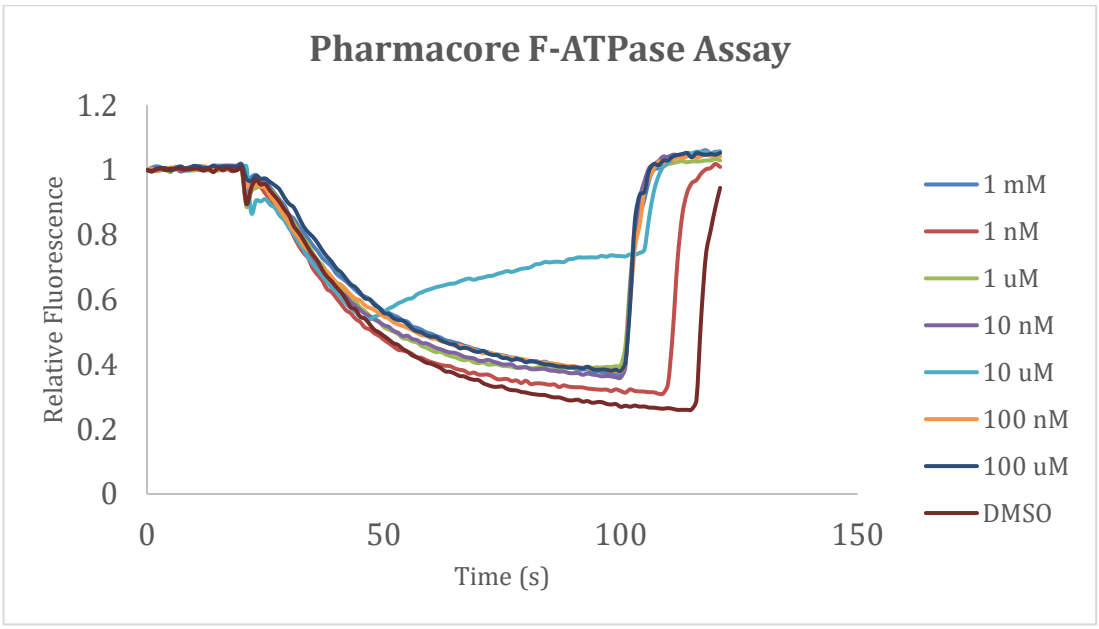
Pharmacore F-ATPase Assay
Relative Fluorescence
1.2
1
0.8
0.6
0.4
0.2
0
0
50
100
150
Time (s)
1 mM
1 nM
1 uM
10 nM
10 uM
100 nM
100 uM
DMSO

b)

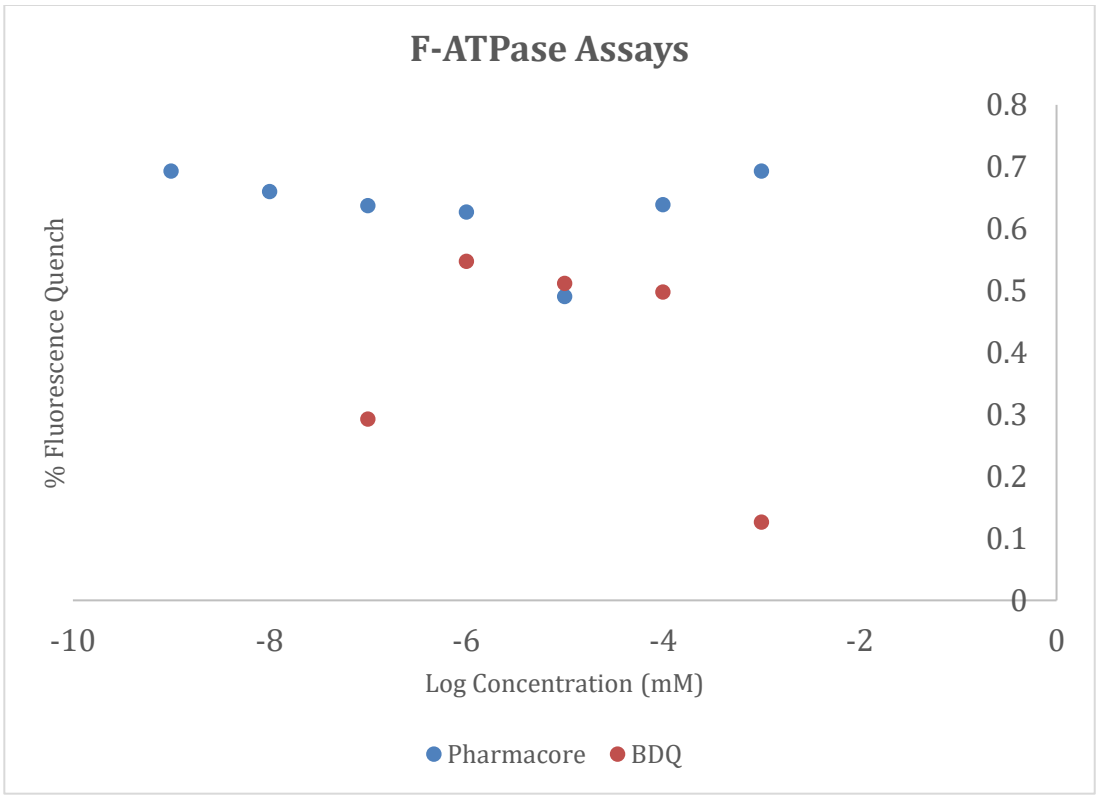


c)

Figure 6. F-ATPase assay of BDQ and base pharmacore.

Figure 6 (a) BDQ F-ATPase assay used to establish a control. (b) Analog 1 F-ATPase assay. (c) Comparison of the control to pharmacore. Results show that pharmacore had no significant inhibitory potential.

## 4. Conclusion

By continual trial-and-error, the systematic methodology development for the base pharmacore was successfully accomplished. The methoxy and dimethylamine substitutions were synthesized and characterized with relative ease. However, the synthetic and purification issues of the Grignard addition were a large stumbling block for the progress of this study. Eventually, synthesis, purification, and characterization of the Grignard product was achieved; thereby, paving the way for future analogs to be synthesized and tested for potential antibiotic activity. Considering the differences in amino acid sequences, said future analogs will incorporate different functional groups to determine how the difference in the hydroxyl group's position in conjunction with steric effects will change *E. coli's* F-ATPase binding affinity (Figure 9). Carbon chains (**10, 11**) and a large aromatic group (**7**) will be added to determine the effects of hydrophobicity and sterics while possible polar interference will be established with an oxidation of the hydroxy group (**8**). A quinoline diamer will be synthesized as quinolines have been found to hold strong anti-bacterial properties (**7**).[14] Computational docking cannot be pursued as there are no high-resolution models of *E. coli's* F-ATPase. Other analogs focusing on the methoxy group are being done by another researcher in tandem.

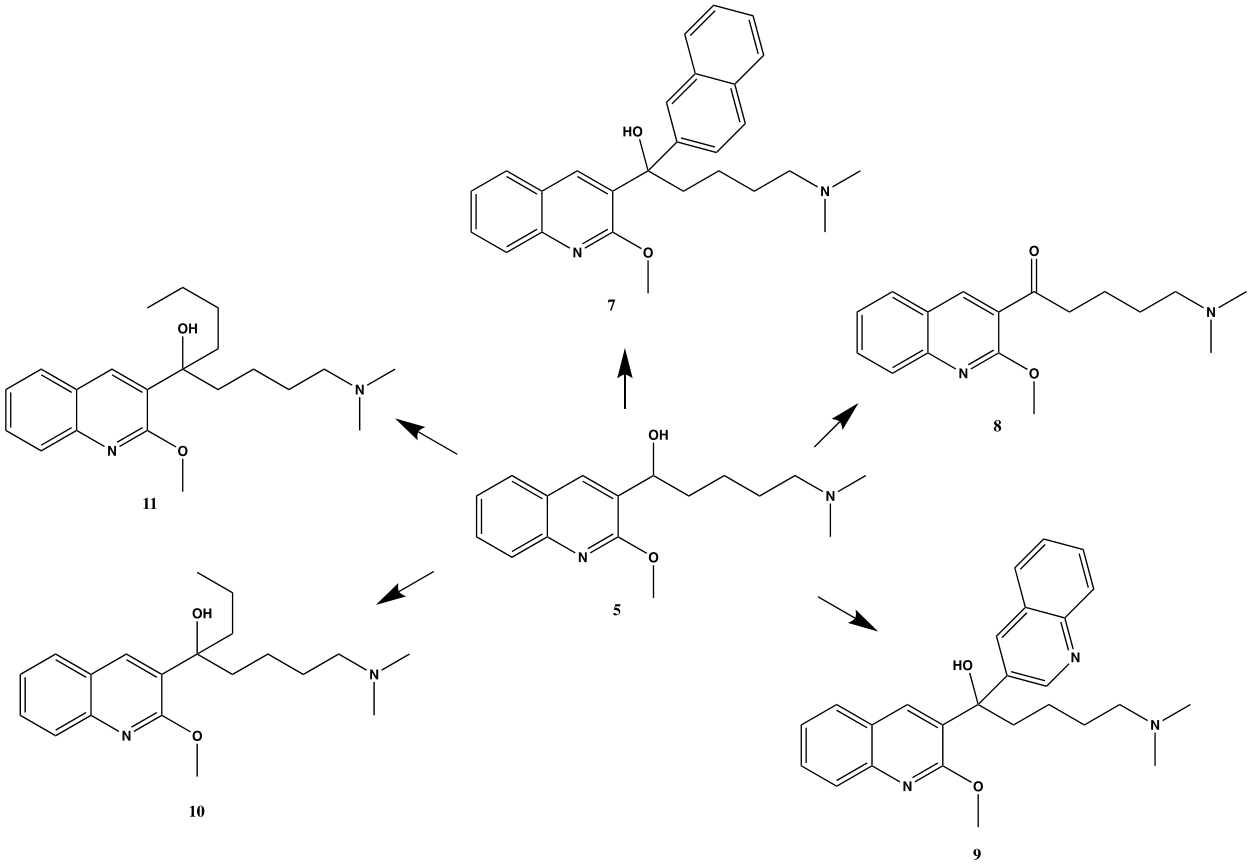


Figure 7. Proposed future analogs.

Figure 7. The addition of carbon chains may help reduce steric conflict (**10,11**), while large aromatic groups might increase binding through stronger hydrophobic interactions (**9**). A quinoline diamer is potentially very toxic and requires further research into its effects (**7**).

## 5. Experimental

All products were confirmed through Hydrogen-NMR (H-NMR), Carbon[13]-NMR (C-NMR), IR, and LC-MS.

### *5.1. 2-Methoxyquinilone-3-carboxaldehyde* (**2**)[15]

2-Chloro-quinilone 3-carboxyaldehyde (0.783 mmol) was added to a solution of 1.5 eq. KOH (1.175 mmol) in MeOH (37.5 mL) and warmed to reflux for 24 h. The solution was cooled to room temperature and DI water (37.5 mL) was added. The organic solvent was removed under vacuum to obtain a precipitate, which was then filtered, washed with $H_2O$ and with $Et_2O$, and dried with anhydrous $Na_2SO_4$. Product was then concentrated under vacuum again to afford a white-yellowish solid (0.0952 g, 69.49%).

### *5.2. 1-(Bromobutyl)pyrrolidine* (**5**)*/Bromo-4-Dimethylaminobutane* (**6**)[10]

Dimethlamine (19.48 mmol) was added to 5 eq. of 1-Bromo-4-chlorobutane (58.45 mmol) in DMF (18 mL) and $K_2CO_3$ (3.3 g) and reflux for 24 h. The reaction mixture was cooled to RT, and the $K_2CO_3$ was filtered out. Sixty mL of $H_2O$ was added and organic layer was extracted using DCM 3 x 30 mL (bottom layer). Dry and filter bottom layer with $Na_2SO_4$. Air dried overnight (O/N). Purification was done through column chromatography (100 EA:0 Hex). Product is a dark coppery color liquid (density: 1.5645 g/mL, 0.3129 g, 9.92%).

### *5.3. 5-(dimethylamino)-1-(2-methoxyquinolin-3-yl)pentan-1-ol* (**3**)/*5-chloro-1-(2-methoxyquinolin-3-yl)pentan-1-ol* (**4**)[16]

Reaction and preparation was done under dry conditions. Preparation: 1-Bromo-4-chlorobutane (14.27 mmol) was added to a 40 mL THF, 0.3467 g Mg° turings, and a catalytic amount of cat. $I_2$ and stirred at RT for 20 min. 2-chlor-quinilone-3-carboxyaldehyde (**2**) (2.830 mmol) was added to a cooled flask (0 °C) and 5 mL THF. Reaction: The starting materials were added and reaction was warmed to RT and run for 3 h. Poured into conc. $NH_4Cl$ and extracted $NH_4Cl$ layer. Extracted organic layer with ethyl acetate 3 x 25 mL. Air dried overnight. Purification was done through column chromatography (100 EA:0 Hex). Product was a yellow-brownish solid.

### 5.4. One Pot: *5-(dimethylamino)-1-(2-methoxyquinolin-3-yl)pentan-1-ol* (**4**)[16]

Reaction and preparation was done under dry conditions. Preparation: 1-Bromo-4-chlorobutane (14.27 mmol) was added to a 40 mL THF, 0.3467 g Mg° turings, and a catalytic amount of cat. $I_2$ and stirred at RT for 20 min. 2-chlor-quinilone-3-carboxyaldehyde (**2**) (2.830 mmol) was added to a cooled flask (0 °C) and 5 mL THF. Reaction: The starting materials were added and reaction was warmed to RT and run for 3 h.
A solution of 50 mL DMF, 4.6 g $K_2CO_3$, and 0.4842 mL dimethylamine was prepared and warmed at 70°C for 30 min. Gringnard product was added directly to prepared solution and run at RT for 24 hrs under $N_2$ atm. Filtered out $K_2CO_3$ and added 150 mL sat. $NH_4Cl$. Extracted organic layer then extracted again with 3x30 mL ethyl acetate (EA). Air dried overnight. Purification through column chromatography (70 EA/30 Hexane (Hex)).

### 5.5 Acid-Base Work-up: *5-chloro-1-(2-methoxyquinolin-3-yl)pentan-1-ol* (**4**).

Under dry conditions, 0.266 mL 1-Bromo-3-chloropropane (2.57 mmol), Mg°, and catalytic $I_2$ to 4 mL dry THF stirring in a RB-flask and cooled to 0 °C for 30 min. Allowed flask to warm to RT for 40 min. Added 2-chlor-quinilone-3-carboxyaldehyde (**2**, 0.857 mmol) and cooled to 0 °C for 20 min, then allowed flask to return to RT over 30 min. Rxn was stopped with 10 mL EA and extracted 3x30 mL sat. $NaHCO_3$. Added 1M HCl until pH <4. Extracted with 3x30 mL EA and air-dried O/N. Purification was done via crystallization.

### *5.6 Fluorescent ATP-driven $H^+$ Pumping Assay*[13]

Wild-type (WT) 160μL of 10 mg/mL ISO vesicles were added to a solution of 3.2 mL HMK buffer (50 mM HEPES, 5 mM MgCl2, 300 mM KCl, pH 7.5), 8 μL ACMA (9-amino-6-chloro-2-methoxyacridine), and 9 μL of inhibitive compound. Excitation and emission wavelengths were set at 415 nm and 485 nm respectively. Voltage levels were auto-ranged for each individual sample (750-950 V). Using an AMINCO Bowman Series 2 Luminescence Spectrometer, fluorescence levels were monitored and recorded. Assay was run for a total of 120 s with 30 μL ATP being injected at 20 s and 8 μL Nigericin at 100 s.

## 6. Acknowledgments

The author wishes to expression their appreciation to the Dr. Amanda L. Wolfe, Dr. P. Ryan Steed, the department of chemistry, the University of North Carolina at Asheville, and funding from the RSCA Cottrell grant.

## 7. References

1. Center for Disease Control. Antibiotic Resistance Threats in the United States, 2013. https://www.cdc.gov/drugresistance/threat-report-2013/pdf/ar-threats-2013-508.pdf#page=13 (accessed Sep 16, 2018).
2. Center for Disease Control. Antibiotic/Antimicrobial Resistance (AR/AMR), 2018.
3. Koonin, E. V., Makarova, K. S., & Aravind, L. Horizontal Gene Transfer in Prokaryotes: Quantification

and Classification. *Annu. Rev. Microbiol.* **2001**, *55*, 709–742.
4. Diffen. Gram-positive vs. Gram-negative Bacteria https://www.diffen.com/difference/Gram-negative_Bacteria_vs_Gram-positive_Bacteria (accessed Nov 4, 2016).
5. Center for Disease Control. Tuberculosis: Data and Statistics https://www.cdc.gov/tb/statistics/default.html (accessed Feb 19, 2018).
6. Andries, K.; Verhasselt, P.; Guilemont, J.; Göhlmann, H.W.H.; Neefs, J.M.; Winkler, H.; Gestel, J.V.; Timmerman, P.; Zhu, M.; Lee, E.; Williams, P.; Chaffoy, D.d.; Heuitric, E.; Hoffner, S.; Cambau, E.; Truffot-Pernot, C.; Lounis, N.; Jarlier, A. A Diarylquinoline Drug Active on the ATP Synthase of Mycobacterium Tuberculosis. *Science (80-. ).* **2005**, *307*, 223–227.
7. Preiss, L.; Langer, J. D.; Yildiz, Ö.; Eckhardt-Strelau, L.; Guillemont, J. E. G.; Koul, A.; Meier, T. Structure of the Mycobacterial ATP Synthase Forotor Ring in Complex with the Anti-TB Drug Bedaquiline. *Sci. Adv.* **2015**, *1* (4), 1–8.
8. Hards, K.; Robson, J. R.; Berney, M.; Shaw, L.; Bald, D.; Koul, A.; Andries, K.; Cook, G. M. Bactericidal Mode of Action of Bedaquiline. *J. Antimicrob. Chemother.* **2015**, *70* (7), 2028–2037.
9. He, C.; Preiss, L.; Wang, B.; Fu, L.; Wen, H.; Zhang, X.; Cui, H.; Meier, T.; Yin, D. Structural Simplification of Bedaquiline: The Discovery of 3-(4-(N,N-Dimethylaminomethyl)Phenyl)Quinoline-Derived Antitubercular Lead Compounds. *ChemMedChem* **2017**, *12* (2), 106–119.
10. Tanwar, B.; Kumar, A.; Yogeeswari, P.; Sriram, D.; Chakraborti, A. K. Design, Development of New Synthetic Methodology, and Biological Evaluation of Substituted Quinolines as New Anti-Tubercular Leads. *Bioorganic Med. Chem. Lett.* **2016**, *26* (24), 5960–5966.
11. Okuno, D.; Iino, R.; Noji, H. Rotation and Structure of FoF1-ATP Synthase. *J. Biochem.* **2011**, *149* (6), 655–664.
12. Nakanishi-Matsui, M.; Sekiya, M.; Nakamoto, R. K.; Futai, M. The Mechanism of Rotating Proton Pumping ATPases. *Biochim. Biophys. Acta - Bioenerg.* **2010**, *1797* (8), 1343–1352.
13. Steed, P. R.; Kraft, K. A.; Fillingame, R. H. Interacting Cytoplasmic Loops of Subunits *a* and *c* of *Escherichia Coli* $F_1F_0$ ATP Synthase Gate $H^+$ Transport to the Cytoplasm. *Proc. Natl. Acad. Sci.* **2014**, *111* (47), 16730–16735.
14. Patterson, R. D. Quinolone Toxicity: Methods of Assessment. *Am. J. Med.* **1991**, *91* (6), 35–37.
15. Waghray, D.; Zhang, J.; Jacobs, J.; Nulens, W.; Basarić, N.; Meervelt, L. Van; Dehaen, W. Synthesis and Structural Elucidation of Diversely Functionalized 5,10-Diaza[5]Helicenes. *J. Org. Chem.* **2012**, *77* (22), 10176–10183.
16. Jain, P. P.; Degani, M. S.; Raju, A.; Anantram, A.; Seervi, M.; Sathaye, S.; Ray, M.; Rajan, M. G. R. Identification of a Novel Class of Quinoline-Oxadiazole Hybrids as Anti-Tuberculosis Agents. *Bioorganic Med. Chem. Lett.* **2016**, *26* (2), 645–649.
17. Koul, A.; Dendouga, N.; Vergauwen, K.; Molenberghs, B.; Vranckx, L.; Willebrords, R.; Ristic, Z.; Lill, H.; Dorange, I.; Guillemont, J.; Bald, D.; Andries, K. Diarylquinolines target subunit c of mycobacterial ATP synthase. *Nature Chemical Biology.* 2007, **3**, 323-324.
18. Haasma, A.C.; Abdillahi-Ibrahim, R.; Wagner, M.J.; Krab, K.; Vergauwen, K.; Guillemont, J.; Andries, K.; Lill, H.; Bald, K. Selevtivity of TMC207 toward Mycbacterial ATP Synthase Compared with That toward the Eukaryotic Homologue. *Antibacterial Agents and Chemotherapy.* 2009, **53** (3), 1290-1292.
19. Fregni, V.; Casadio, R. Kinetic characterization of the ATP-dependent proton pump in bacterial photosynthetic membranes: a study with fluorescent probe 9-amino-6-chloro-2-methoxyacridine. *BBA – Bioenergetics.* 1993. **1143** (2), 215-222.
20. Mahendar, L.; Satyanarayana, G. Substitution Controlled Functionalized *othro*-Bromobenzylic Alcohols via Palladium Catalyst: Synthesis of Chromenes and Indenols. *Journal of Organic Chemistry*. 2014, ***79***, 2059-2074.
21. Penefsky HS. Mechanism of inhibition of mitochondrial adenosine triphosphatase by dicyclohexylcarbodiimide and oligomycin: relationship to ATP synthesis. *Proceedings of the National Academy of Sciences of the United States of America*. 1986, ***82***, 1589-1593.
22. Hornback, J. M. *Organic Chemistry*, 2nd ed.; Thompson. Brooks. Cole: 2005.
23. Priebbenow, D.L.; Barbaro, L.; Baell, J.B. New syntehetic approaches towards analogues of Bedaquiline. *Org. Biomol Chem.* 2016, **14,** 9622.
24. Tanwar, B.; Kumar, A.; Yogeeswari, P.; Sriram, D.; Chakraborti, A. K. Design, development of new synthetic methodology, and biological evaluation of substituted quinolines as new anti-tubercular leads. *Bioorganic & Medicinal Chemistry Letters*. 2016, ***26***, 5960-5966.
25. Qiao, C.J.; Wang, X.K.; Xie, F.; Zhong, W.; Li, S. Asymmetric Synthesis and Absolute Configuration Assignment of a New Type of Bedaquiline Analogue. *Molecules*. 2015, ***20***, 22272-22285.

26. Krebs, Jocelyn E.; Goldstein, Elliot S.; Kilpatrick, Stephen T. Lewin's Genes XII. Jones. Barlett. 2017.
27. Fu, LM.; Fu-Liu, CS. Is Mycobacterium tuberculosis a closer relative to Gram-positive or Gram-negative bacterial pathogens? *Tuberculosis*. 2008, ***82***, 85-90.